Virologica Sinica 38 (2023) 975–979

Contents lists available at ScienceDirect

Virologica Sinica

journal homepage: www.keaipublishing.com/en/journals/virologica-sinica
www.virosin.org

Letter

Structural insight into EV-A71 3A protein and its interaction with a peptide inhibitor

Yahui Liu [a,1], Panjing Lv [a,1], Wei Wang [b], Jiahai Zhang [c], Xi Zhou [d], Yang Qiu [d], Kun Cai [e,*], Haoran Zhang [a,*], Yuan Fang [d,*], Yan Li [a,f,*]

[a] Department of Pathogen Biology, School of Basic Medicine, Tongji Medical College and State Key Laboratory for Diagnosis and Treatment of Severe Zoonotic Infectious Diseases, Huazhong University of Science and Technology, Wuhan, 430030, China
[b] Medical Subcenter of HUST Analytical & Testing Center, Huazhong University of Science and Technology, Wuhan, 430030, China
[c] MOE Key Laboratory for Membraneless Organelles and Cellular Dynamics, School of Life Sciences, Division of Life Sciences and Medicine, University of Science and Technology of China, Hefei, 230027, China
[d] State Key Laboratory of Virology, Wuhan Institute of Virology, Chinese Academy of Sciences, Wuhan, 430071, China
[e] Institute of Health Inspection and Testing, Hubei Provincial Center for Disease Control and Prevention (Hubei CDC), Wuhan, 430079, China
[f] Department of Pediatrics, Tongji Hospital, Tongji Medical College, Huazhong University of Science and Technology, Wuhan, 430030, China

Dear Editor,

Hand, foot, and mouth disease (HFMD) is a common illness among children that is usually mild and self-limiting. However, in some severe cases, patients may rapidly develop neurological and systemic complications that can be fatal (Ooi et al., 2010). HFMD is caused by a few serotypes of human enterovirus A (HEV-A) species (Yu and Cowling, 2019), with enterovirus A71 (EV-A71) and coxsackievirus A16 (CV-A16) being the most typical causative agents (Yu and Cowling, 2019). Furthermore, severe neurological sequelae are more common in cases with EV-A71 serotype infection than other serotypes (Ooi et al., 2010; Yu and Cowling, 2019). There has been a significant increase in EV-A71 epidemic activity throughout the Asia–Pacific region (McMinn, 2002) since EV-A71 was first isolated from a patient with central nervous system (CNS) disease in 1969 (Schmidt et al., 1974).

EV-A71 is a small non-enveloped virus belonging to HEV-A species of the genus *Enterovirus* in the family *Picornaviridae* (Nasri et al., 2007). Its genome is a single-stranded positive-sense RNA of approximately 7400 bp in length and contains only one complete open reading frame (ORF), which encodes a large polyprotein (Solomon et al., 2010). The polyprotein is eventually hydrolyzed into four structural proteins (VP1–VP4), which form the viral icosahedral capsid and enclose the viral genome, and seven non-structural proteins (2A–2C and 3A–3D) (Mandary and Poh, 2018). Although several EV-A71 inactivated vaccines are now available for HFMD prevention (Guan et al., 2020; Mao et al., 2016; Nguyen et al., 2022), no antiviral drugs with replication inhibition effects against EV-A71 have progressed to the clinical trial stage as complementary therapies to these vaccines. Notably, the viral non-structural proteins are considered potential targets for antiviral drug development due to their critical roles in viral replication, pathogenesis, and immune evasion (Norder et al., 2011).

Similar to other positive-strand RNA viruses, enteroviruses replicate their viral genomes by remodeling the intracellular membranes of host cells and assembling viral replication organelles (ROs) (Salonen et al., 2005). The non-structural protein 3A of EV-A71 has been identified to recruit the lipid kinase phosphatidylinositol 4-kinase IIIβ (PI4KB) to the ROs and facilitates viral replication by binding to a host factor, acyl-CoA-binding domain-containing protein 3 (ACBD3) and promoting PI4KB-ACBD3 interaction (Xiao et al., 2017). Recently, a novel host factor, secretory carrier membrane protein 3 (SCAMP3), has also been shown to associate with enterovirus 3A protein, PI4KB, and phosphatidylinositol-4-phosphate (PI4P) to form replication complexes and participate in viral replication (Lu et al., 2021). It has also been shown that 3A protein interacts with proteins such as host neuronal PRSS3 (brain trypsinogen) and vacuolar protein sorting 25 to facilitate viral replication (Rattanakomol et al., 2022; Ruan et al., 2022). Together, the crucial role of 3A protein in viral replication highlights its potential as a target for drug development.

Spanning residues 1441–1526 within the polyprotein, EV-A71 3A protein is a small membrane-anchoring protein containing 86 amino acids and forms homodimers to function (Horova et al., 2019). It includes a transmembrane domain near the C-terminus, and two amphipathic α-helices near the N-terminus serving as the homodimerization interface (Horova et al., 2019). Structures of dimeric 3A protein in several Enterovirus species complexed with ACBD3 GOLD domain have been resolved, including EV-A71 (PDB: 6HLW) (Horova et al., 2019), EV-G1 (PDB: 6Q69) (Smola et al., 2020) and EV-F2 (PDB: 6Q68) (Smola et al., 2020). Despite the high conservation within the two amphipathic

* Corresponding authors.
E-mail addresses: ckreal@163.com (K. Cai), hrzhang@outlook.com (H. Zhang), fangyuan_125@163.com (Y. Fang), yanli@hust.edu.cn (Y. Li).
[1] Yahui Liu and Panjing Lv contributed equally to this work.

https://doi.org/10.1016/j.virs.2023.09.004
Received 7 July 2023; Accepted 22 September 2023
Available online 26 September 2023

α-helices (Supplementary Fig. S1A), the dimerization patterns of these 3A proteins displayed both similarities and discrepancies: EV-G1 and EV-A71 3A dimers are most similar (Supplementary Fig. S1B), while EV-F2 forms a differently oriented 3A dimer (Supplementary Fig. S1C), depicting a varied interspecies homodimerization landscape. Recently, Qiu et al. have shown that the EV-A71 3A protein acts as a viral suppressor of RNAi (VSR), a host innate antiviral immunity mechanism that involves post-transcriptional gene silencing (Qiu et al., 2017). Furthermore, ER-DRI, a D-peptide designed to target the dimerization interface of EV-A71 3A protein to inactive its VSR function, showed potent anti-enteroviral efficacies against EV-A71 both *in vitro* and *in vivo* by restoring the RNAi response in infected host cells (Fang et al., 2021). ER-DRI has also demonstrated potent antiviral activity against CV-A16, which also contains homodimeric 3A protein as well, indicative of the potential for designing pan-anti-enteroviral drugs using a strategy to disrupt the homodimeric interface of 3A protein. However, the underlying molecular mechanisms of 3A-ER-DRI interaction remain unclear, limiting the future development of ER-DRI-based drugs.

In this study, we present a comprehensive characterization of the structural, biophysical, and biochemical profiles of the EV-A71 3A protein. Utilizing nuclear magnetic resonance (NMR) spectroscopy and molecular docking methods, we further disclosed key mechanisms for the interaction between the D-peptide ER-DRI and EV-A71 3A protein. Our results provided insights into the interaction interface and mechanisms of ER-DRI in inhibiting the dimeric state of EV-A71 3A protein, laying an important foundation for optimizing and improving the design of subsequent anti-enteroviral therapeutic peptides.

To enhance the expression level of soluble EV-A71 3A protein, we fused a 6×His-tag, and a SUMO-tag at the N-terminus of the extracellular domain of 3A protein to create the construct 6×His-SUMO-$3A_{1–57}$. This construct was then used for later biophysical interaction studies and structural investigations since the standalone expression of the extracellular domain ($3A_{1–57}$) in *E. coli* expression system presents poor solubility (Horova et al., 2019). The detailed method is in the Supplementary Materials. The 6×His-SUMO-$3A_{1–57}$ was expressed and cleaved with SUMO protease to generate a recombinant $3A_{1–57}$ protein (comprising 63 aa) with a theoretical isoelectric point (pI) of 5.27 and a calculated molecular weight of 7.16 kDa. The recombinant $3A_{1–57}$ protein was eventually homogenized via size-exclusion chromatography (Supplementary Fig. S2A and S2B). The elution volume is close to the position of a dimer, which implies that the recombinant $3A_{1–57}$ protein should be dimeric in solution. We performed a ^{1}H NMR experiment and confirmed that the $3A_{1–57}$ protein was well-folded in solution, as evidenced by the sharp amide ^{1}H peaks distributed at 6.5–9.0 ppm (Supplementary Fig. S2C). The purified $3A_{1–57}$ protein was then used for follow-up experiments.

We next prepared uniformly [^{13}C,^{15}N]-labeled $3A_{1–57}$ protein samples for further heteronuclear NMR characterizations. The backbone resonance assignments of $3A_{1–57}$ were obtained by regular backbone three-dimensional spectra analysis. Totally, 75% (42/56) of the backbone amide ^{1}H–^{15}N pairs were assigned to the non-proline amino acids of $3A_{1–57}$ protein (Fig. 1A). In particular, the peak intensities of residues 25–45 (residues 1459–1479 in EV-A71 polyprotein) were significantly lower compared to those of other residues, presumably reflecting the homodimer formation involving this fragment as elucidated by the previously resolved $3A_{1–57}$ crystal structure (PDB: 6HLW) (Horova et al., 2019). Leveraging $C_O/H_N/N/C_\alpha/C_\beta$ chemical shift assignments, we predicted the secondary structure of $3A_{1–57}$ with TALOS-N (Shen and Bax, 2013). Notably, $3A_{1–57}$ in solution exhibits similar secondary structural elements to the crystal structure 6HLW, where residues 25–45 exhibit a tendency to form two helical structures (Fig. 1B). This is in accordance to the putative homodimerization state of 3A in solution as the amphipathic helices are expected to cluster in water solution in an entropy-driven way. In addition, we noticed that except for the unassigned I49, E58, R59, and H60, chemical shift-based predictions revealed that residues 46–63 are a structurally disordered region (Supplementary Fig. S3). In contrast, the fragment TNVERH (residues 49–54 in 6HLW or residues 55–60 in this study) in the holo-form crystal structure (PDB: 6HLW) (Horova et al., 2019) is β-stranded and forms an anti-parallel β-sheet with other β-strands of the ACBD3 GOLD domain. Since the NMR data in our study was acquired with apo-form $3A_{1–57}$ samples, this discrepancy in secondary structure elements implicates potential target binding-driven β-strand formation for the fragment TNVERH of EV-A71 $3A_{1–57}$, depicting a dynamic process during the binding by ER-DRI.

With the majority of backbone assignments of EV-A71 $3A_{1–57}$ protein, we conducted NMR ^{15}N relaxation analysis to further investigate the structural dynamics of $3A_{1–57}$. Longitudinal relaxation rate R_1, transverse relaxation rate R_2, and {^{1}H}-^{15}N heteronuclear steady-state nuclear Overhauser effect (hNOE) values for individual residues were obtained from ^{15}N relaxation measurements (Fig. 1C–E). We analyzed a total of 37 non-proline residues, excluding those with overlapped peaks or low signal-to-noise ratios. Residues 1–24 and 50–63, located at the N- and C-terminals of $3A_{1–57}$, respectively, are highly dynamic as evidenced by their low R_2 and hNOE values (<0.6). This observation agrees with our chemical shift-based secondary structure prediction (Fig. 1B) where the C-terminal residues adopt the form of a disordered coil in apo state instead of a β-strand like in ACBD3-complexed state. Meanwhile, as expected, the helix motif (residues 25–46) showed less flexibility with low R_1, high R_2, and high hNOE values. Of note, residues D25, A26, and E37 displayed significantly higher R_2 values than other helical residues, implicating in possible conformational exchange for these residues. Given that these three residues are not in direct contact with another monomeric unit within the EV-A71 3A homodimer, as shown in the crystal structure, the possible conformational exchange might reflect a distinct dynamics pattern of the protein in solution. Overall, these results confirmed the two relative rigid helices and the flexible loops in both termini in solution.

Furthermore, using the T_1/T_2 data of residues 25–46, the relative rigid region of EV-A71 $3A_{1–57}$, we calculated the rotational correlation time τ_c to be 10.49 ns. An empirical formula reported by Rossi (Rossi et al., 2010) was then used to estimate the apparent molecular weight (M_w) of EV-A71 $3A_{1–57}$ as 16.78 kDa. This result supports the dimeric state of the 7.16-kDa $3A_{1–57}$ protein in solution, where the statistical deviation can be attributed to the dimerization equilibrium process as well as the complex overall motion pattern brought about by disordered regions at both termini.

To probe the detailed molecular interactions between EV-A71 and ER-DRI, ^{1}H–^{15}N HSQC spectra were recorded and analyzed for ^{15}N-labeled EV-A71 $3A_{1–57}$ protein in the presence of serial unlabeled ER-DRI, with the molar ratios between EV-A71 $3A_{1–57}$ and ER-DRI set to 1:0, 1:2, 1:4 and 1:8 (Fig. 1F and G). Notably, the α-helix motif of $3A_{1–57}$ protein exhibits line broadening in the ^{1}H–^{15}N HSQC spectrum upon ER-DRI titration, indicative of ER-DRI binding to the dimeric interface with intermediate chemical exchange (near micromolar binding affinity) (Teilum et al., 2017), which is comparable to the results of previous research reporting submicromolar K_D and IC_{50} values [K_D: 0.059 μmol/L; IC_{50}: 0.45 μmol/L in RD cells and 0.79 μmol/L in Vero cells against EV-A71 strain H (VR-1432) infection] (Fang et al., 2021). The dimerization surface of the $3A_{1–57}$ protein contains most of the residues that are affected by the ER-DRI titration, such as I21, D23, L24, D29, S30, C37, D39, and Q40 (named I27, D29, L30, D35, S36, C43, D45, and Q46 in Fig. 1F due to indexed expression tag sequence for NMR studies; Fig. 1H–J). Of note, these residues engage in hydrophobic clustering (I21, L24), hydrogen bonds (D23, S30, D39), and electrostatic interactions (D29) within an amphipathic α-helix chain or with the α-helix from the other monomer according to the holo-form crystal structure (Fig. 1H), and putatively provide geometric complementarity across the dimerization interface (Fig. 1I). This suggests that the ER-DRI peptides disrupt the formation of $3A_{1–57}$ protein dimers required for its full functionality, partially explaining the peptide's potent inhibition efficacy against the EV-A71. Furthermore, the high sequential conservation of these binding active sites across related

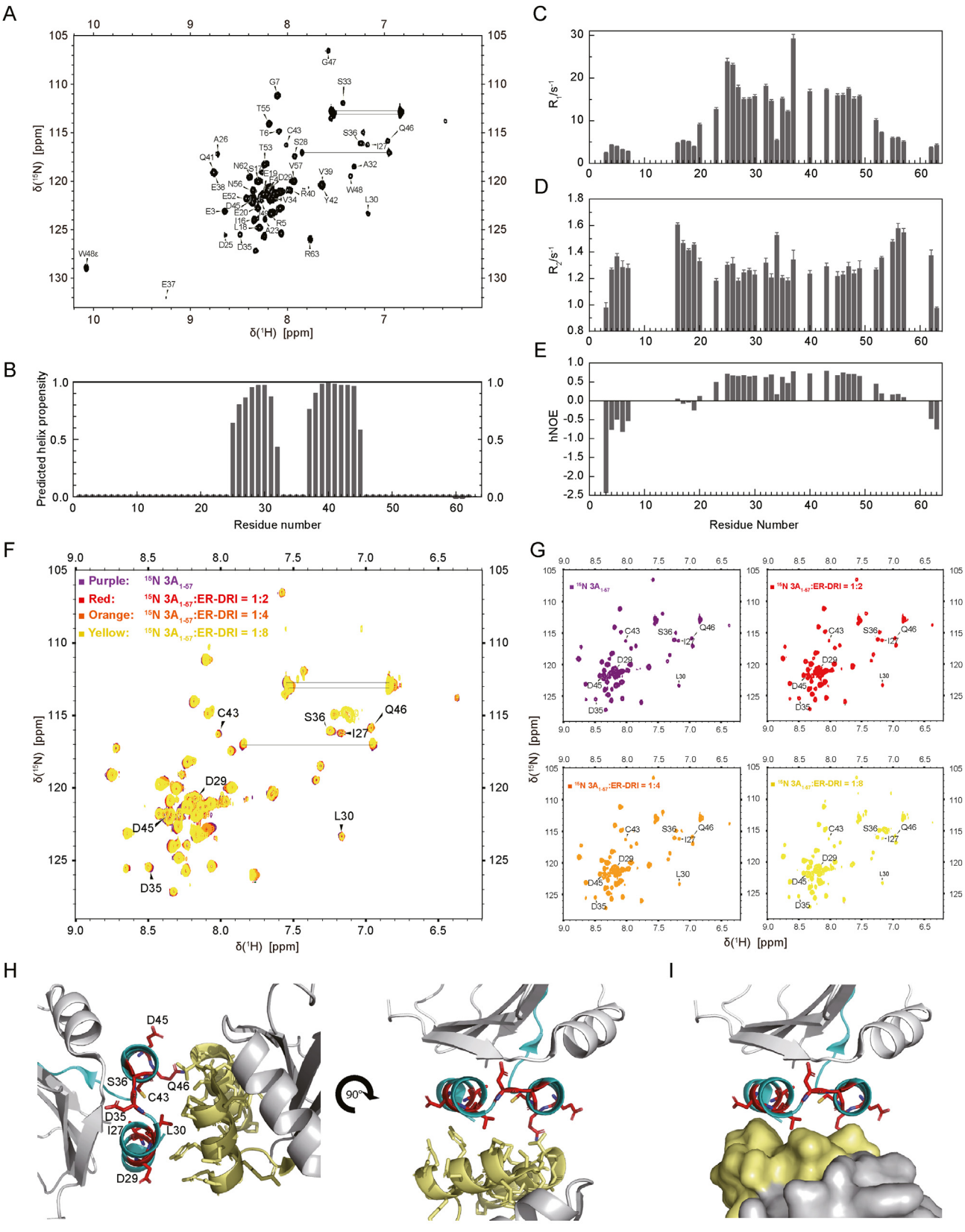

(caption on next page)

Fig. 1. Nuclear magnetic resonance (NMR) characterization of structural and inhibitor-binding properties of EV-A71 $3A_{1–57}$ protein. **A** Backbone resonance assignments of EV-A71 $3A_{1–57}$ shown in $^{1}H–^{15}N$ HSQC spectrum. Assigned cross-peaks are labeled with their single-letter residue name and residue number. **B** Secondary structure prediction of EV-A71 $3A_{1–57}$ based on TALOS-N (Shen and Bax, 2013). The possibility (0–1) predicted based on chemical shift for each residue to be helical is plotted. **C–E** NMR ^{15}N relaxation analysis of EV-A71 $3A_{1–57}$ protein. The relaxation parameters R_1 (**C**), R_2 (**D**), and hNOE (**E**) are indicated in column graphs. **F** Overlay of $^{1}H–^{15}N$ HSQC spectra of 100 μmol/L ^{15}N-labeled $3A_{1–57}$ in the absence (purple) and presence of increasing amounts of D-peptide ER-DRI in natural abundance (molar ratio at 1:2, red; 1:4, orange; 1:8, yellow, respectively). **G** Separate $^{1}H–^{15}N$ HSQC spectra for (**F**). **H** Mapping the EV-A71 $3A_{1–57}$ residues with line broadening upon titration by small-molecule inhibitor ER-DRI (in red) to the crystal structure of EV-A71 3A (PDB: 6HLW). The two 3A monomers in the heterotetramer are colored in cyan and yellow, respectively. **I** Same as the left panel of (**H**), with the yellow 3A monomer shown as surface. **J** The multiple sequence alignment among the EV-A71 3A protein (the third row) and its homologs, including 3A protein of coxsackievirus-A16 (the first row), hypothetical protein EHQ45_11580 of *Leptospira bourretii* (the second row), and 3A protein of EV-A120 (the fourth row).

species like CV-A16, *Leptospira bourretii* and EV-A120 (Fig. 1J) hints a possible expansion of ER-DRI usage in a broad-spectrum way as an anti-pathogen drug after further optimization and preclinical/clinical trials. Sequence alignment between *L. bourretii* and Enterovirus demonstrated that residues I21, D23, L24, D29, C37, D39, Q40 are highly conserved across species, suggesting their critical role in dimerization.

Using the residues with significant peak intensity loss as interaction sites, we then conducted molecular docking between $3A_{1–57}$ and ER-DRI. From the 10,000 docking models generated, the complex structure model with the lowest energy was analyzed for ER-DRI-$3A_{1–57}$ binding. Key residues exhibiting the disappearance of signals were mapped onto the docking model (Supplementary Fig. S4). As a result, the residues I21, D23, L24, C37, D39, Q40, which were confirmed by our NMR data (Fig. 1F), were involved in the surface that is influenced by the binding to ER-DRI (Supplementary Fig. S4). This outcome is comparable to the 3A homodimer crystal structure (Fig. 1H and I), indicating a mechanism of competitive inhibition by ER-DRI. Interestingly, although the 3A helix-mimicking part of ER-DRI (rcyqrvee, D-amino acids in a retro-reversed sequence) was designated as active sites during molecular docking, the helix motif of $3A_{1–57}$ was found to bind alternatively to the TAT peptide segment (rrrqrrkkrgy) of ER-DRI. This promotes novel mechanistic insights into the ER-DRI-$3A_{1–57}$ interaction beyond the anticipated mimic-and-compete inhibition process. Further experimental investigation on the binding details of this interaction might be needed to elucidate the target site of $3A_{1–57}$ on ER-DRI.

HFMD is a viral disease mainly caused by infection with enteroviruses, especially EV-A71 and CV-A16. The susceptibility and severity of HFMD have been shown to be age-related, with the majority of cases being diagnosed in children younger than five years of age who tended to cluster and caused herd infection in kindergartens (Zhu et al., 2023). The highly contagious enteroviruses and asymptomatic recessive infections also can facilitate large-scale, difficult-to-control epidemics in a short period of time (Koh et al., 2018). HFMD can lead to HFMD-associated neurological complications such as brainstem encephalitis, aseptic meningitis, cardiopulmonary failure, and even death, although in most cases it is usually mild and self-limiting (Jones et al., 2018). EV-A71 is a neurotropic virus and there is a positive correlation between the EV-A71 viral load and the severity of CNS (Wang et al., 2023). Unfortunately, there is currently no specific medical treatment for EV-A71. While certain inactivated vaccines are available against EV-A71, their long-term efficacy remains unproven (Lim and Poh, 2019). Therefore, advancing research and development of clinically available therapies against EV-A71 is crucial for the effective treatment of HFMD and should be prioritized as a matter of urgency. The life cycle of EV-A71 is similar to most viruses and includes attachment, entry, decapitation, replication, translation, assembly, and viral release from host cells (Baggen et al., 2018). The non-structural 3A protein takes part in the formation of replication complexes, which are involved in the early life cycle of EV-A71 (Horova et al., 2019). Apart from a few agents, such as itraconazole and the enviroxime-like compounds (Gao et al., 2015), there is still a lack of effective drugs targeting 3A for the treatment of EV-A71 infection. Therefore, further attention and research are warranted on the potential of EV-A71-targeting drugs for this purpose.

In this study, we successfully prepared the extracellular domain of the 3A protein of EV-A71 and characterized the folding of $3A_{1–57}$ with the ^{1}H NMR analysis. Subsequently, we assigned 75% of non-proline residues of $3A_{1-57}$ protein by collecting and analyzing the three-dimensional spectra of the [^{13}C,^{15}N]-labeled $3A_{1–57}$ protein. Consequently, we performed a dynamic analysis of the ^{15}N-labeled $3A_{1–57}$ protein, and the estimated M_w of $3A_{1–57}$ based on T_1 and T_2 data indicates that $3A_{1–57}$ is presumably present in solution as a dimer. Finally, we performed a set of titration experiments of ^{15}N-labeled $3A_{1–57}$ protein with ER-DRI, which was previously reported could directly bind to 3A protein and thereby block EV-A71 replication (Fang et al., 2021), to investigate the details of ER-DRI binding to $3A_{1–57}$ protein. ER-DRI was designed as the antagonist against the dimer of 3A protein, specifically targeting the α-helix motif. The titration results are consistent with previous speculations that ER-DRI is able to bind to the α-helix motif, thus preventing the formation of 3A protein dimerization. We also performed a docking of ER-DRI and $3A_{1–57}$ protein.

Here, we illustrated the protein-inhibitor binding pattern by which the replication of EV-A71 can be effectively inhibited by the 3A-targeting peptide ER-DRI. ER-DRI shows significant intermolecular interactions with the homodimer interface of the 3A protein, which should competitively block the dimerization by the 3A α-helix motif. In addition, since the 3A protein is not only a highly conserved non-structural protein in the *Enterovirus* genus, but also a common feature of several other pathogens, including *Leptospira* and coxsackievirus (Fig. 1J). By elucidating the structural basis of how the peptide binds and inhibits the 3A protein, we have opened up new possibilities for designing and optimizing more potent inhibitors against these diseases.

Footnotes

This work was funded by the National Key Research and Development Program of China (2021YFC2600200 to Y.L.), the National Natural Science Foundation of China (82172299 to Y.L., and 82172269 to Y.Q.), the Hubei Provincial Nature Science Foundation (2020CFB516 to K.C.), the Hubei Provincial Public Health Outstanding Young Talents Project (to Y.L. and K.C.), the Hubei Province Natural Science Foundation for Distinguished Young Scholars (2022CFA068 to Y.L.) and the Open Research Fund Program of the State Key Laboratory of Virology of China (2022KF001 to K.C.). Xi Zhou is an editorial board member for *Virologica Sinica* and was not involved in the editorial review or the decision to publish this article. The authors declare no competing interests.

Supplementary data to this article can be found online at https://doi.org/10.1016/j.virs.2023.09.004.

References

Baggen, J., Thibaut, H.J., Strating, J.R.P.M., van Kuppeveld, F.J.M., 2018. The life cycle of non-polio enteroviruses and how to target it. Nat. Rev. Microbiol. 16, 368–381.

Fang, Y., Liu, Z., Qiu, Y., Kong, J., Fu, Y., Liu, Y., Wang, C., Quan, J., Wang, Q., Xu, W., Yin, L., Cui, J., Xu, Y., Curry, S., Jiang, S., Lu, L., Zhou, X., 2021. Inhibition of viral suppressor of RNAi proteins by designer peptides protects from enteroviral infection in vivo. Immunity 54, 2231–2244.e6.

Gao, Q., Yuan, S., Zhang, C., Wang, Ying, Wang, Yizhuo, He, G., Zhang, S., Altmeyer, R., Zou, G., 2015. Discovery of itraconazole with broad-spectrum in vitro antienterovirus activity that targets nonstructural protein 3A. Antimicrob. Agents Chemother. 59, 2654–2665.

Guan, X., Che, Y., Wei, S., Li, S., Zhao, Z., Tong, Y., Wang, L., Gong, W., Zhang, Y., Zhao, Y., Wu, Y., Wang, S., Jiang, R., Huang, J., Liu, Y., Luo, W., Liao, Y., Hu, X., Zhang, W., Dai, Y., Jiang, G., Min, G., Liu, F., You, X., Xu, X., Li, J., Li, C., Fan, S., Hang, L., Huang, Q., Li, Q., 2020. Effectiveness and safety of an inactivated enterovirus 71 vaccine in children aged 6–71 months in a phase IV study. Clin. Infect. Dis. 71, 2421–2427.

Horova, V., Lyoo, H., Różycki, B., Chalupska, D., Smola, M., Humpolickova, J., Strating, J.R.P.M., van Kuppeveld, F.J.M., Boura, E., Klima, M., 2019. Convergent evolution in the mechanisms of ACBD3 recruitment to picornavirus replication sites. PLoS Pathog. 15, e1007962.

Jones, E., Pillay, T.D., Liu, F., Luo, L., Bazo-Alvarez, J.C., Yuan, C., Zhao, S., Chen, Q., Li, Y., Liao, Q., Yu, H., Rogier van Doorn, H., Sabanathan, S., 2018. Outcomes following severe hand foot and mouth disease: a systematic review and meta-analysis. Eur. J. Paediatr. Neurol. 22, 763–773.

Koh, W.M., Badaruddin, H., La, H., Chen, M.I.C., Cook, A.R., 2018. Severity and burden of hand, foot and mouth disease in Asia: a modelling study. BMJ Glob. Health 3, e000442.

Lim, H.X., Poh, C.L., 2019. Insights into innate and adaptive immune responses in vaccine development against EV-A71. Ther. Adv. Vaccines Immunother. 7, 2515135519888998.

Lu, J.Y., Brewer, G., Li, M.L., Lin, K.Z., Huang, C.C., Yen, L.C., Lin, J.Y., 2021. Secretory carrier membrane protein 3 interacts with 3A viral protein of enterovirus and participates in viral replication. Microbiol. Spectr. 9, e00475-21.

Mandary, M.B., Poh, C.L., 2018. Changes in the EV-A71 genome through recombination and spontaneous mutations: impact on virulence. Viruses 10, 320.

Mao, Q., Wang, Y., Bian, L., Xu, M., Liang, Z., 2016. EV71 vaccine, a new tool to control outbreaks of hand, foot and mouth disease (HFMD). Expert Rev. Vaccines 15, 599–606.

McMinn, P.C., 2002. An overview of the evolution of enterovirus 71 and its clinical and public health significance. FEMS Microbiol. Rev. 26, 91–107.

Nasri, D., Bouslama, L., Pillet, S., Bourlet, T., Aouni, M., Pozzetto, B., 2007. Basic rationale, current methods and future directions for molecular typing of human enterovirus. Expert Rev. Mol. Diagn. 7, 419–434.

Nguyen, T.T., Chiu, C.H., Lin, C.Y., Chiu, N.C., Chen, P.Y., Le, T.T.V., Le, D.N., Duong, A.H., Nguyen, V.L., Huynh, T.N., Truong, H.K., Phan, T.L., Nguyen, T.T.T., Shih, S.R., Huang, C.G., Weng, Y.J., Hsieh, E.F., Chang, S., Chen, C., Tai, I.C., Huang, L.M., 2022. Efficacy, safety, and immunogenicity of an inactivated, adjuvanted enterovirus 71 vaccine in infants and children: a multiregion, double-blind, randomised, placebo-controlled, phase 3 trial. Lancet 399, 1708–1717.

Norder, H., De Palma, A.M., Selisko, B., Costenaro, L., Papageorgiou, N., Arnan, C., Coutard, B., Lantez, V., De Lamballerie, X., Baronti, C., Solà, M., Tan, J., Neyts, J., Canard, B., Coll, M., Gorbalenya, A.E., Hilgenfeld, R., 2011. Picornavirus non-structural proteins as targets for new anti-virals with broad activity. Antiviral Res. 89, 204–218.

Ooi, M.H., Wong, S.C., Lewthwaite, P., Cardosa, M.J., Solomon, T., 2010. Clinical features, diagnosis, and management of enterovirus 71. Lancet Neurol. 9, 1097–1105.

Qiu, Y., Xu, Y., Zhang, Y., Zhou, H., Deng, Y.Q., Li, X.F., Miao, M., Zhang, Q., Zhong, B., Hu, Y., Zhang, F.C., Wu, L., Qin, C.F., Zhou, X., 2017. Human virus-derived small RNAs can confer antiviral immunity in mammals. Immunity 46, 992–1004.e5.

Rattanakomol, P., Srimanote, P., Tongtawe, P., Khantisitthiporn, O., Supasorn, O., Thanongsaksrikul, J., 2022. Host neuronal PRSS3 interacts with enterovirus A71 3A protein and its role in viral replication. Sci. Rep. 12, 12846.

Rossi, P., Swapna, G.V.T., Huang, Y.J., Aramini, J.M., Anklin, C., Conover, K., Hamilton, K., Xiao, R., Acton, T.B., Ertekin, A., Everett, J.K., Montelione, G.T., 2010. A microscale protein NMR sample screening pipeline. J. Biomol. NMR 46, 11–22.

Ruan, Z., Liang, Y., Chen, Z., Yin, J., Li, C., Pan, P., Zhang, Q., Wu, J., Luo, Z., 2022. Enterovirus 71 non-structural protein 3A hijacks vacuolar protein sorting 25 to boost exosome biogenesis to facilitate viral replication. Front. Microbiol. 13, 1024899.

Salonen, A., Ahola, T., Kääriäinen, L., 2005. Viral RNA replication in association with cellular membranes. In: Marsh, M. (Ed.), Membrane Trafficking in Viral Replication. Springer Berlin Heidelberg, Berlin, Heidelberg, pp. 139–173.

Schmidt, N.J., Lennette, E.H., Ho, H.H., 1974. An apparently new enterovirus isolated from patients with disease of the central nervous system. J. Infect. Dis. 129, 304–309.

Shen, Y., Bax, A., 2013. Protein backbone and sidechain torsion angles predicted from NMR chemical shifts using artificial neural networks. J. Biomol. NMR 56, 227–241.

Smola, M., Horova, V., Boura, E., Klima, M., 2020. Structural basis for hijacking of the host ACBD3 protein by bovine and porcine enteroviruses and kobuviruses. Arch. Virol. 165, 355–366.

Solomon, T., Lewthwaite, P., Perera, D., Cardosa, M.J., McMinn, P., Ooi, M.H., 2010. Virology, epidemiology, pathogenesis, and control of enterovirus 71. Lancet Infect. Dis. 10, 778–790.

Teilum, K., Kunze, M.B.A., Erlendsson, S., Kragelund, B.B., 2017. (S)Pinning down protein interactions by NMR. Protein Sci. 26, 436–451.

Wang, S., Pang, Z., Fan, H., Tong, Y., 2023. Advances in anti-EV-A71 drug development research. J. Adv. Res. S2090-1232(23)89-9.

Xiao, X., Lei, X., Zhang, Z., Ma, Y., Qi, J., Wu, C., Xiao, Y., Li, L., He, B., Wang, J., 2017. Enterovirus 3A facilitates viral replication by promoting phosphatidylinositol 4-kinase IIIβ–ACBD3 interaction. J. Virol. 91, e00791-17.

Yu, H., Cowling, B.J., 2019. Remaining challenges for prevention and control of hand, foot, and mouth disease. Lancet Child Adolesc. Health 3, 373–374.

Zhu, P., Ji, W., Li, D., Li, Z., Chen, Y., Dai, B., Han, S., Chen, S., Jin, Y., Duan, G., 2023. Current status of hand-foot-and-mouth disease. J. Biomed. Sci. 30, 15.